AD-A138 377 A SUMMARY OF WHISTLERS OBSERVED BY VOYAGER 1 AT JUPITER 1/1
(U) IOWA UNIV IOWA CITY DEPT OF PHYSICS AND ASTRONOMY
W S KURTH ET AL. 20 DEC 83 U. OF IOWA-83-31
UNCLASSIFIED N00014-76-C-0016 F/G 3/2 NL

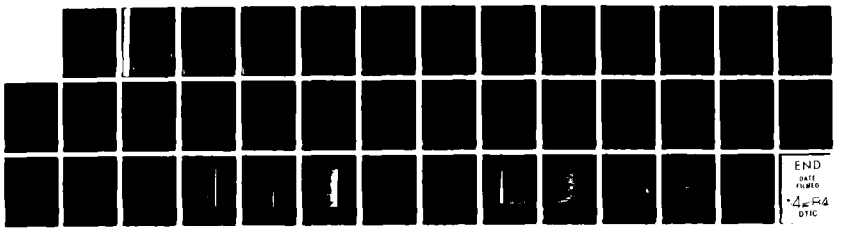

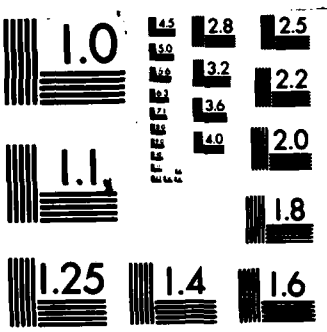


MICROCOPY RESOLUTION TEST CHART
NATIONAL BUREAU OF STANDARDS-1963-A

U. of Iowa 83-

AD A138377

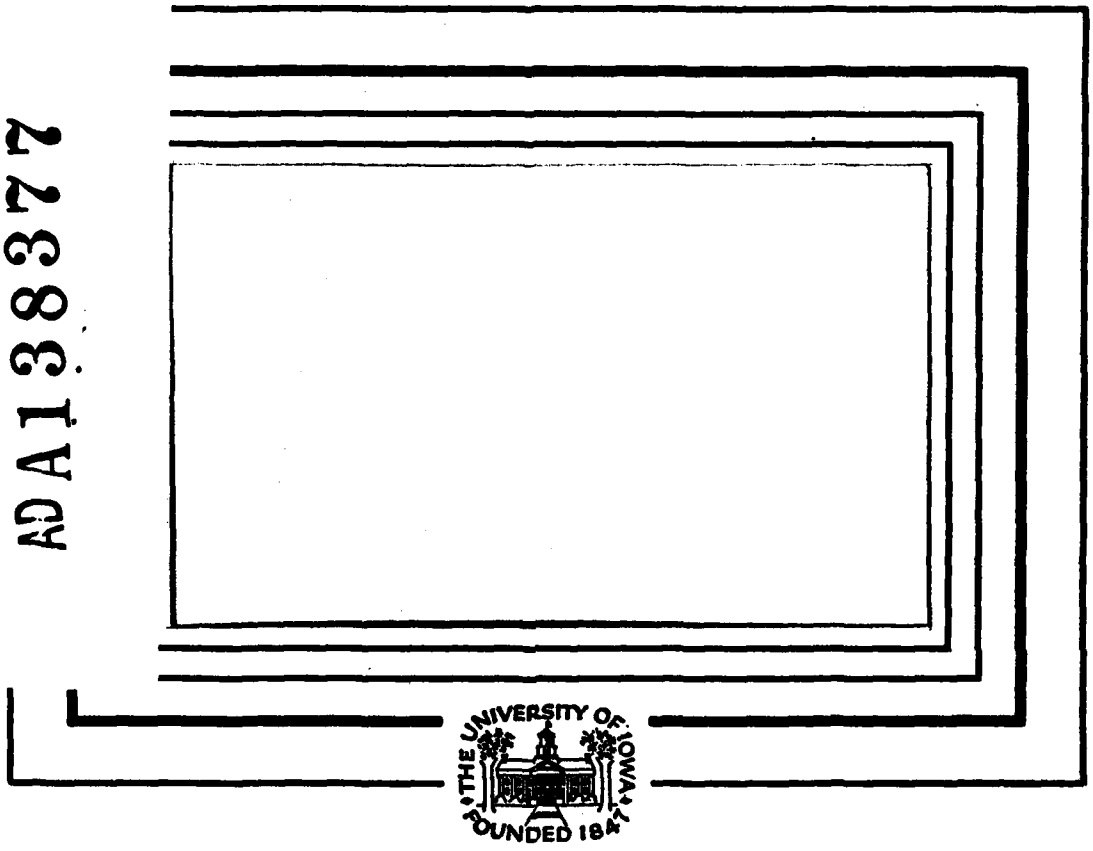


DTIC FILE COPY

DTIC ELECTE FEB 28 1984 D

A

Department of Physics and Astronomy

# THE UNIVERSITY OF IOWA

Iowa City, Iowa 52242



84 02 28 036

U. of Iowa 83-31

# A Summary of Whistlers Observed by Voyager 1 at Jupiter

by

W. S. Kurth[1], B. D. Strayer[1], D. A. Gurnett[1], and F. L. Scarf[2]

December 1983

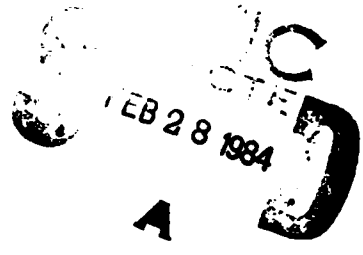


Submitted to the Journal of Geophysical Research.

[1]Department of Physics and Astronomy, The University of Iowa, Iowa City, Iowa 52242

[2]TRW Space and Technology Group, One Space Park, Redondo Beach, California 90278

The research at the University of Iowa was supported by the National Aeronautics and Space Administration through Grant NAGW-337 and through Contract 954013 with the Jet Propulsion Laboratory, and by the Office of Naval Research through Grant N00014-76-C-0016. The research at TRW was supported by NASA through Contract 954012 with the Jet Propulsion Laboratory.

UNCLASSIFIED

SECURITY CLASSIFICATION OF THIS PAGE (When Data Entered)

| REPORT DOCUMENTATION PAGE | | READ INSTRUCTIONS BEFORE COMPLETING FORM |
|---|---|---|
| 1. REPORT NUMBER<br>U. of Iowa 83-31 | 2. GOVT ACCESSION NO.<br>AD-A138377 | 3. RECIPIENT'S CATALOG NUMBER |
| 4. TITLE (and Subtitle)<br>A SUMMARY OF WHISTLERS OBSERVED BY VOYAGER 1 AT JUPITER | | 5. TYPE OF REPORT & PERIOD COVERED<br>Progress, December 1983<br>6. PERFORMING ORG. REPORT NUMBER |
| 7. AUTHOR(s)<br>W. S. KURTH, B. D. STRAYER, D. A. GURNETT and F. L. SCARF | | 8. CONTRACT OR GRANT NUMBER(s)<br>N00014-76-C-0016 |
| 9. PERFORMING ORGANIZATION NAME AND ADDRESS<br>Department of Physics and Astronomy<br>The University of Iowa<br>Iowa City, IA 52242 | | 10. PROGRAM ELEMENT, PROJECT, TASK AREA & WORK UNIT NUMBERS |
| 11. CONTROLLING OFFICE NAME AND ADDRESS<br>Office of Naval Research<br>Electronics Program Office<br>Arlington, VA 22217 | | 12. REPORT DATE<br>20 December 1983<br>13. NUMBER OF PAGES<br>37 |
| 14. MONITORING AGENCY NAME & ADDRESS(if different from Controlling Office) | | 15. SECURITY CLASS. (of this report)<br>15a. DECLASSIFICATION/DOWNGRADING SCHEDULE |

16. DISTRIBUTION STATEMENT (of this Report)

Approved for public release; distribution is unlimited.

17. DISTRIBUTION STATEMENT (of the abstract entered in Block 20, if different from Report)

18. SUPPLEMENTARY NOTES

Submitted to the Journal of Geophysical Research

19. KEY WORDS (Continue on reverse side if necessary and identify by block number)

Whistlers
Lightning
Jupiter

20. ABSTRACT (Continue on reverse side if necessary and identify by block number)

(See abstract following)

DD FORM 1 JAN 73 1473 EDITION OF 1 NOV 65 IS OBSOLETE
S/N 0102-LF-014-6601

UNCLASSIFIED
SECURITY CLASSIFICATION OF THIS PAGE (When Data Entered)

## ABSTRACT

We summarize the Voyager 1 observations of whistlers at Jupiter in order to provide a basis for further analyses of the density profile of the Io plasma torus as well as to support studies of atmospheric lightning at Jupiter. All the whistlers detected by Voyager 1 fell into three general regions in the torus at radial distances ranging between 5 and 6 $R_J$. An analysis of the broadband wave amplitudes measured by the Voyager 1 plasma wave instrument and estimates of the peak whistler amplitudes imply the grouping of whistlers was due to variations in the sensitivity of the receiver to whistlers and not to variations in the source or propagation paths of the whistlers. The whistler dispersions are presented in statistical form for each of the three groups of events and analyzed in view of the structure of the Io plasma torus as determined by plasma probe measurements. The results of these analyses give source locations for the whistlers at the foot of the magnetic field lines threading the torus in both hemispheres and over a range of longitudes.


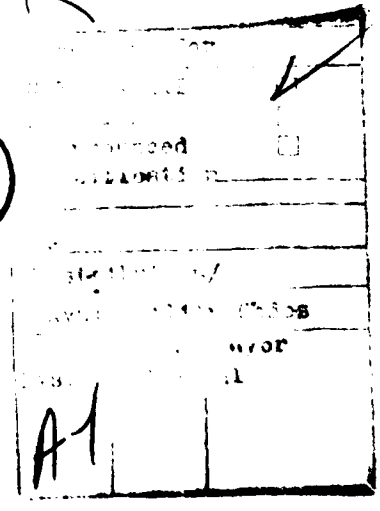

# I. INTRODUCTION

The discovery of whistlers at Jupiter [Gurnett et al., 1979; Scarf et al., 1979] gave conclusive proof of the existence of atmospheric lightning at that planet [Smith et al., 1979]. Hence, Jupiter became the second planet exhibiting lightning activity besides the Earth. Ksanfomaliti et al. [1979] and Taylor et al. [1979] presented evidence of lightning at Venus in the form of electromagnetic noise bursts at low frequencies. More recently, Kaiser et al. [1983] have interpreted Saturn electrostatic discharges at high frequencies as evidence for lightning in the atmosphere of Saturn.

A considerable amount of work has already been completed utilizing the whistler observations at Jupiter to ascertain some information on the distribution of plasma along the magnetic field lines connecting the lightning source to the spacecraft [Gurnett et al., 1979; Gurnett et al., 1981; Tokar et al., 1982a,b]. Other work has been reported which uses the rate of whistler detection to arrive at lightning flash rates in the Jovian atmosphere [Lewis, 1980; Scarf et al., 1981b].

In order to support further work in both the study of the distribution of plasma in the Io torus as well as estimates of the lightning flash rates we will provide a detailed summary of all whistlers observed at Jupiter. The whistler activity was confined to three general periods of time while Voyager 1 was within the Io plasma torus. We shall characterize each of these three groups by the average

dispersion of the whistlers and the number of whistlers detected. One new and interesting result will be to show that the grouping of whistler activity is apparently controlled by the level of other in-band signals which controls the gain of the receiver and not by clumpiness in the source of the whistlers or by variations in the propagation medium.

The Voyager plasma wave instrument is described fully by Scarf and Gurnett [1977]; however, we shall summarize the characteristics which are important in this study for the convenience of the reader. The plasma wave receiver consists of a multichannel spectrum analyzer and a wideband waveform receiver which are each connected to a balanced electric dipole antenna with two 10-m elements oriented perpendicular to each other. The spectrum analyzer provides low temporal and spectral resolution measurements over the frequency range from 10 Hz to 56.2 kHz with a dynamic range of about 100 dB below 100 $mVm^{-1}$. The waveform receiver provides very high resolution waveform measurements in the frequency range of 40 Hz to 12 kHz. The waveform receiver has an automatic gain control (AGC) which maintains a nearly constant output amplitude independent of the input signal strength over a dynamic range of about 100 dB. The time constant of the AGC is 0.25 s. The waveform measurements are converted from an analog signal to 4 bit digital words at a rate of 28,800 $s^{-1}$. The four-bit digitization yields a dynamic range for the waveform measurements of about 23 dB. The waveform data are Fourier analyzed on the ground to provide the frequency-time spectrograms shown herein.

## II. OBSERVATIONS

Whistlers have a unique frequency-time structure which allows them to be identified easily in a frequency-time spectrogram. Figure 1 shows several examples of whistlers detected by the Voyager 1 plasma wave instrument during its closest approach to Jupiter in March 1979. The format for the spectrograms is intensity (darkness, where the most intense waves are black) as a function of frequency (ordinate) and time (abscissa). The two whistlers in Figure 1a show best the characteristic decrease in frequency with increasing time of these emissions. This structure is due to the dispersion of whistler mode waves in a plasma and was first described by Eckersley [1935] as

$$t = D/\sqrt{f} + t_o \quad , \tag{1}$$

where t is the arrival time of a wave at frequency, f, and D is the dispersion constant. For the first whistler in the top panel of Figure 1 D = 290 $s\sqrt{Hz}$. The second whistler has a dispersion constant of 275 $s\sqrt{Hz}$. The several whistlers seen in Figure 1b have much smaller dispersions than the two in Figure 1a, typically 45 $s\sqrt{Hz}$. The whistlers in Figure 1c show the largest dispersions observed at Jupiter, ~ 500 $s\sqrt{Hz}$.

A visual survey of the wideband spectrograms obtained over about a nine-hour interval near closest approach was carried out in order to identify all the whistlers detected by Voyager. Figure 2 shows the trajectory of Voyager 1 in the magnetic meridian plane containing the spacecraft as it traversed the Io torus on 5 March, 1979. During the period between about 0615 and 1510 SCET (spacecraft event time) a total of 141 48-s wideband frames were available for analysis, representing a duty cycle of about 21%. During the remaining 79% of the time from 0615 to 1510 SCET no wideband data were obtained because the high speed downlink was being used to transmit images. The three regions in the trajectory denoted by a heavy line and identified by the letters A, B, and C are intervals when whistlers were visible in the spectrograms. The examples in Figures 1a, 1b, and 1c represent each of these three regions. A total of 167 whistlers were identified in the data. Of these, 77 lacked sufficient extent in frequency and time to allow reliable dispersion determination and, hence, were not included in the study.

Figure 3 summarizes the location (in time), frequency range, and dispersion of the 90 whistlers which had sufficient spectral and temporal extent to provide a measure of dispersion. At the top of Figure 3 the time of each of the 141 wideband frames is denoted by a tick mark. Obviously, nothing can be said about the occurrence of whistlers during periods when no wideband data are available. The spectrum analyser data is not adequate to allow reliable identification of whistlers without the use of wideband data [Scarf et al., 1981a]. The top panel in Figure 3 illustrates the frequency range and number of

whistlers detected as a function of time. Note that no whistlers were found prior to 0900 SCET or after 1512 SCET. The numbers in the top panel refer to the number of whistlers detected within a 40-second interval represented by the line at that time. The vertical extent of the line represents the range in frequency between the average low and high frequency limits of the whistlers occurring during the appropriate 40-s interval.

The dispersion constant was measured for each of the whistlers. For the low dispersion whistlers of region B, the dispersion was measured simply by overlaying transparencies of the Eckersley formula with different values for D until a good match was made. By covering the range of 20 to 100 $s\sqrt{Hz}$ in 5-$s\sqrt{Hz}$ intervals in the overlays, it was possible to measure D to within 2 $s\sqrt{Hz}$, or about 3% accuracy. For the higher dispersion whistlers of regions A and C a number of measurements of f and t were obtained to arrive at an average value of D for each whistler with standard deviations of about 2%. We note here that although the Eckersley formulation is an approximation, Menietti and Gurnett [1980] have shown it is quite accurate over the frequency range utilized here.

The bottom panel of Figure 3 summarizes the dispersions of the whistlers. The average dispersion for the whistlers within each 40-s averaging interval is plotted with an error bar denoting one standard deviation. The three regions of whistler activity identified in Figure 2 are most clearly distinguishable in the dispersion summary. Clearly, the whistlers detected in region B have the smallest dispersions of any of the three groups, averaging near 70 $s\sqrt{Hz}$, while

whistlers in regions A and C have larger dispersions. Whistlers in region A have dispersions near 250 $s\sqrt{Hz}$ and region C whistlers have dispersions of about 500 $s\sqrt{Hz}$. The histogram of dispersions in Figure 4 shows these three populations. Note that on a linear scale the region C dispersions form a rather loosely bound population, yet, it is still distinguishable from the other two populations. The different dispersions of these three groups of whistlers has been used by Tokar et al. [1982b] to determine whether the lightning sources are located in the northern or southern hemisphere.

An estimate of the peak amplitude of the whistlers was obtained by displaying the Fourier transform of single 60-msec sweeps of the waveform data as in Figure 5. The difficulty here is that the AGC circuitry does not directly allow for absolute amplitude determination because the instantaneous gain of the AGC is not known. The calibration process, then, is a two-fold procedure. The first step is to generate a plot of spectral density as a function of frequency as in Figure 5, but in arbitrary units. The second step involves plotting the calibrated spectral density from the spectrum analyzer at the appropriate time (assuming the spectrum of the background noise is relatively constant over the 4-s accumulation time) to the same scale and sliding the two plots until a good match is obtained over as large a frequency range as possible. The result is a spectrum calibrated in absolute units as in Figure 5.

A difficulty with the above described procedure is that the accumulation time for a spectrum has to be kept to a minimum so as to not smear out the whistler as its frequency shifted. Unfortunately, a

spectrum obtained in such a short period of time (60 msec) is very noisy and it is often difficult to differentiate between the noise and the whistler signal. The result is that very few whistlers were found which showed a reasonable signal-to-noise ratio. This is not a problem in dynamic spectra as in Figure 1 since the eye can easily discern the characteristic whistler trace in the frequency-time format even though the amplitude at any one given time is barely above the noise background.

Spectral densities in the form of Figure 5 were obtained for the two region A whistlers shown in Figure 10. Peak intensities were obtained by multiplying the peak spectral density by one-half the bandwidth at half maximum and taking the square root. For the first whistler in Figure 10, the peak intensity is 27 $\mu Vm^{-1}$ at 3.3 kHz. The peak intensity of the second whistler at 4.5 kHz is 39 $\mu Vm^{-1}$. It would be more appropriate to integrate over the entire whistler to give an integrated power, however, the signal is not strong enough to provide sufficient reliability over the frequency range observed, plus the entire range of frequencies emitted by a lightning stroke is obviously not observed.

Consideration of Figure 3 leads to the question of why there are three distinct groups of whistlers and large intervals of time in between during which no whistlers were detected. It might seem reasonable to speculate that Voyager is simply seeing the "clumpiness" in the location of thunderstorms in the atmosphere or variations in propagation paths which are alternately favorable and unfavorable for low-loss propagation. An alternate possibility is that the receiver sensitivity

to whistlers varies as a function of time (or space) and that there is no real variation in whistler occurrence rates. We have investigated the latter possibility in some detail and the result is shown in Figure 6.

The top panel of Figure 6 simply shows the number of whistlers detected in each 48-s frame of wideband data. Dots representing zero occurrence rates denote frames which are available for study but which show no whistlers. Hence, the top panel shows not only the whistler rate as a function of time, but also the coverage of the wideband receiver. The key parameter which determines the sensitivity of the wideband receiver is the broadband signal strength over the passband of the receiver (40 Hz to 12 kHz) since it is this signal which sets the receiver gain via the AGC. Using the spectrum analyzer data, we have integrated the electric field intensities from the 56-Hz channel to the 10-kHz channel, correcting for the finite bandwidth of those channels, and plotted the resulting broadband electric field strength in the bottom panel of Figure 6.

Given that the instantaneous dynamic range afforded by the 4 bit analog-to-digital converter is about 23 dB and the receiver gain is set to provide about 6 dB "head room", one can construct a time-varying envelope of the dynamic range as indicated by the shaded region in the lower panel which extends 6 dB above and 17 dB below the trace of the broadband electric field strength. The interesting point to notice is that a line set at 30 $\mu Vm^{-1}$ representing the peak whistler intensities lies above the receiver threshold (or lower bound of the dynamic range envelope) in the three time intervals corresponding almost exactly with

regions A, B, and C. The peak whistler intensity also exceeds the receiver threshold for a few periods between ~ 1315 and 1415 SCET, however, there are no wideband frames in that time interval, hence, no whistlers were detected.

It is quite clear from Figure 6 that the regions of whistler activity are determined solely by the variation of receiver sensitivity due to changes in the background broadband signal strength. This does not preclude the possibility that there are localized regions where the occurrence of whistlers is enhanced for physical reasons, however, the existence of such regions cannot be established from the Voyager 1 data.

## III. SOURCE LOCATIONS AND PROPAGATION PATHS

In this section we investigate the source location of the whistlers and discuss the implications of the dispersion of the whistlers for the propagation path of the waves. In a sense, this is a circular discussion, since the dispersion is based on the integrated density along the wave trajectory and a determination of the source location depends somewhat on the distribution of density in the Io plasma torus. The situation is not as hopeless as it might seem, however, since some a priori knowledge of the torus structure is available from an analysis of the planetary radio astronomy data [Birmingham et al., 1981] as well as from plasma probe observations [Bagenal and Sullivan, 1981]. The treatment is then more of an iterative one where using existing information on the torus density leads to a source location for the whistlers which, in turn, can yield more accurate information on the torus density structure [see, for example, Tokar et al., 1982a].

Both Jupiter and Io provide conditions which might support lightning discharges. The fascinating storm systems visible in the Voyager images of Jupiter [Smith et al., 1979] are obvious candidates for sources of lightning and images shown in Cook et al. [1979] reveal the presence of lightning discharges on the nightside. Io, however, with its volcanos must also be considered a possible source. It has long been known that lightning is associated with volcanic activity on

Earth and recently evidence for lightning associated with volcanos on Venus has been reported [Scarf and Russell, 1983].

For regions A and B it is easy to eliminate Io as the source of the observed whistlers since the whistler mode waves are constrained to propagate within 19° of the magnetic field line. For the first two regions of activity, Io was at a different longitude than Voyager and only Jupiter was within the 19° cone. Both Jupiter and Io were within the cone during the time the region C whistlers were detected. The intensities of the region C whistlers were no greater than those in the other regions and one would expect much larger intensities if the source were on Io which was only ~ 20,000 km away at the time. The short distance to Io would also require extremely large densities between Voyager 1 and Io to account for the large dispersion of the region C whistlers if the source were on Io. We conclude, then, that the source of all whistlers detected was Jupiter.

To determine from which hemisphere of Jupiter the whistlers came requires some knowledge of the structure of the Io torus. Figure 7 shows the trajectory of Voyager 1 and the three regions of whistler activity superimposed on a model of the Io torus given by Bagenal et al. [1980]. Referring back to the bottom panel of Figure 3 and the histogram of Figure 4 it has been shown that the three regions of whistler activity are differentiated most clearly by their dispersion. Gurnett et al. [1979] have shown that D is proportional to the integrated plasma frequency along the ray trajectory

$$D \approx \frac{1}{2c} \int \frac{f_p}{\sqrt{f_g}} \, ds \qquad (2)$$

where $f_p$ and $f_g$ are the electron plasma frequency and gyrofrequency and c is the speed of light (see also, Helliwell [1965]). Equation 2 is valid for propagation parallel to the magnetic field assuming the wave frequency $f \ll f_g$ in the limit $ff_g \ll f_p^2$. Since $f_p = 8980\sqrt{n_e}$ ($n_e$ is the electron density), D is proportional to $\sqrt{n_e}$ integrated along the ray trajectory and it is clear the high dispersion whistlers had to traverse a large portion of the torus. The propagation through the ionosphere accounts for only a few percent of the total dispersion [Gurnett et al., 1979].

For region C, which has large dispersions and is located near the southern edge of the torus, it is clear the whistlers had to traverse most of the torus before arriving at the spacecraft indicating a northern hemispheric source. Region B, on the other hand, is typified by relatively short whistlers requiring a trajectory with relatively small columnar densities. Since these whistlers were detected while Voyager was near the northern limit of the cold inner torus, the northern hemisphere, again, seems to be the source. The case for the region A whistlers is not nearly so clean as for the other two. Voyager 1 was very close to the centrifugal equator at this time and the large dispersions could be the result of propagation from either hemisphere.

An analysis by Tokar et al. [1982b] provides some additional insight on the source location of the region A whistlers. They calculated transit times by integrating the group index of refraction along the field line from the source to the spacecraft using heavy ion concentrations measured by the plasma probe to obtain a dispersion. Tokar et al. then determined the concentration of light ions required to match the observed dispersions in region A. Using the path from the northern hemisphere yielded an unacceptably high concentration of light ions, hence, it was concluded the source of the region A whistlers must be in the southern hemisphere. The calculated light ion concentrations for the other two regions are consistent with those in region A, lending a level of credibility to the analysis of Tokar et al.

The source location results are summarized in Figure 8. The dashed lines are the footprints of field lines threading the Io torus mapped onto the cloud-tops. The heavy lines indicate the longitude of the source for each of the three regions assuming parallel propagation. The magnetic field model used here is the $O_4$ model of Acuña and Ness [1976]. Also shown in Figure 8 are the locations of visible lightning activity observed by Voyager 1 on the nightside [Cook et al., 1979].

Given the propagation path, it is possible to derive information on the integrated density along the path and thereby probe the density of the torus and high latitude regions remotely. Considerable work along these lines has been carried out by Tokar et al. [1982a,b] and will not be repeated here. In summary of that work, however, it has been shown that there must be a considerable concentration of light

ions at higher latitudes to account for the dispersion of the observed whistlers. The differentiation of ionic species at varying heights above the centrifugal equator has some interesting implications. The most important of which is a polarization reversal of the ion cyclotron mode predicted by Gurnett and Goertz [1983] and Thorne and Moses [1983]. Ion cyclotron waves are thought to be necessary to scatter energetic heavy ions into the loss cone to account for the intense torus aurora reported by the Voyager ultraviolet instrument [Broadfoot et al., 1979]. Because of the polarization reversal, however, the ion cyclotron mode cannot be observed directly at the latitudes surveyed by Voyager.

The highest observed whistler frequency sets an absolute lower limit to the plasma frequency along the ray path since the whistler mode cannot propagate above $f_p$ [Gurnett et al., 1979]. In the upper panel of Figure 3 one can see that the upper frequency extent of the whistlers varies between about 4 and 7 kHz, corresponding lower limits on the electron density along the paths of 0.2 to 0.6 $cm^{-3}$. This implies dramatic differences in electron densities may exist between the near equatorial and high latitude regions along the same field line since $n_e$ near the equator can be as high as 2000 $cm^{-3}$. Indeed, Tokar et al. [1982a] have shown typical values of $n_e$ near a few to 10 $cm^{-3}$ at high latitudes when the equatorial density is $\sim 10^3$ $cm^{-3}$.

The whistler observations also set an upper bound on the electron temperature of the torus. Menietti and Gurnett [1980] calculated an upper bound by using Landau damping arguments and assuming the

whistlers were nonducted. As a whistler passes through the dense torus the wave normal angle will increase and Landau damping will occur. The lowest cutoff frequency for the region A whistlers was ~ 2 kHz as can be seen in the upper panel of Figure 3. This cutoff corresponds to an upper limit to the temperature in the torus of 2 to 3 × $10^5$ °K. The agreement with the ultraviolet observations of an electron temperature of $10^5$ °K by Broadfoot et al. [1979] is quite good.

## IV. DISCUSSION AND CONCLUSIONS

Studies of the Voyager 1 observations of whistlers at Jupiter have yielded a wealth of information about the occurrence of lightning in the Jovian atmosphere as well as the structure and temperature of the Io plasma torus. Although whistlers were only detected in three rather narrowly confined regions along the Voyager 1 trajectory, it is likely whistlers are common throughout at least the inner portion of the torus since it appears the background plasma wave spectrum masks the detection of whistlers at other times. From the maximum number of whistlers detected within a single 48-s wideband frame of about 32 (see Figure 6) it is clear the whistler rate can approach 1 $s^{-1}$. Evidence is given which locates the lightning activity at the foot of Io torus flux tubes in both hemispheres and over a range of latitudes.

In Figure 8 the locations of bright spots on the nightside of Jupiter found with long exposures by the imaging subsystem are compared with the whistler source locations. Even though the whistler observations do not coincide with the imaging results, there is no reason to doubt either the identification of the bright spots by Cook et al. [1979] or the whistler source regions as lightning. Rather, it is likely the two methods simply observed different lightning sources. In fact, it would have been impossible to detect whistlers which corresponded to the lightning observations of Cook et al. since no

wideband frames were obtained at the proper Jovian longitude and radial distance to detect whistlers from those longitudes.

One of the motivations of this paper is to provide critical observations of whistlers to those who would try to understand the chemistry of the Jovian atmosphere based on energization via lightning discharges. These observations have already led to an estimate of the upper limit to the lightning flash rate on Jupiter of ~ 40 flashes per square kilometer per year [Scarf et al., 1981b]. The upper limit is obtained using an assumption of ducted whistlers which severely restricts the area at the foot of a flux tube which has access to the spacecraft since propagation would be essentially parallel to the magnetic field. Menietti and Gurnett [1980], however, argue that there is little evidence for ducting since no multiple hop whistlers are observed. In the nonducted case, propagation could be at angles up to 19° with respect to a field line and, hence, the area at the foot of the flux tube having access to the spacecraft is greatly expanded and the resulting lightning rate would decrease correspondingly.

## ACKNOWLEDGEMENTS

The research at the University of Iowa was supported by the National Aeronautics and Space Administration through Grant NAGW-337, and through Contract 954013 with the Jet Propulsion Laboratory, and by the Office of Naval Research through Grant N00014-76-C-0016. The research at TRW was supported by NASA through Contract 954012 with the Jet Propulsion Laboratory.

## REFERENCES

Acuña, M. H., and N. F. Ness, Results from the GSFC fluxgate magnetometer on Pioneer 11, in Jupiter, ed. by T. Gehrels, The University of Arizona Press, Tucson, 836, 1976.

Bagenal, F., and J. D. Sullivan, Direct plasma measurements in the Io torus and inner magnetosphere of Jupiter, J. Geophys. Res., 86, 8447, 1981.

Bagenal, F., J. D. Sullivan, and G. L. Siscoe, Spatial distributions of plasma in the Io torus, Geophys. Res. Lett., 7, 41, 1980.

Birmingham, T. J., J. K. Alexander, M. D. Desch, R. F. Hubbard, and B. M. Pedersen, Observations of electron gyroharmonic waves and the structure of the Io torus, J. Geophys. Res., 86, 8497, 1981.

Broadfoot, A. L., M. J. S. Belton, P. Z. Takacs, B. R. Sandel, D. E. Schemansky, J. B. Holberg, J. M. Ajello, S. K. Atreya, T. M. Donahue, H. W. Moos, J. L. Bertaux, J. E. Blamont, D. F. Strobel, J. C. McConnell, A. Dalgarno, R. Goody, and M. B. McElroy, Extreme ultraviolet observations from Voyager 1 encounter with Jupiter, Science, 204, 979, 1979.

Cook, A. F., T. C. Duxbury, and G. E. Hunt, First results on Jovian lightning, Nature, 280, 794, 1979.

Eckersley, J. L., Musical atmospherics, Nature, 135, 104, 1935.

Helliwell, R. A., Whistlers and Related Ionospheric Phenomena, Stanford University Press, Stanford, 35, 1965.

Gurnett, D. A., and C. K. Goertz, Ion cyclotron waves in the Io plasma torus: Polarization reversal of whistler mode noise, Geophys. Res. Lett., 10, 587, 1983.

Gurnett, D. A., F. L. Scarf, W. S. Kurth, R. R. Shaw, and W. S. Kurth, Determination of Jupiter's electron density profile from plasma wave observations, J. Geophys. Res., 86, 8199, 1981.

Gurnett, D. A., R. R. Shaw, R. R. Anderson, and W. S. Kurth, Whistlers observed by Voyager 1: Detection of lightning on Jupiter, Geophys. Res. Lett., 6, 511, 1979.

Kaiser, M. L., J. E. P. Connerney, and M. D. Desch, Atmospheric storm explanation of Saturnian electrostatic discharges, Nature, 303, 50, 1983.

Ksanfomaliti, L. V., N. M. Vasil'chikov, O. F. Ganpantserova, E. V. Petrova, A. O. Souvorov, G. F. Filippov, O. V. Vablonskaya, and L. V. Yabrova, Electrical discharges in the atmosphere of Venus, Pisma Astron. Zh., 5, 229, 1979.

Lewis, J. S., Lightning on Jupiter: Rate, energetics, and effects, Science, 210, 1351, 1980.

Menietti, J. D., and D. A. Gurnett, Whistler propagation in the Jovian magnetosphere, Geophys. Res. Lett., 7, 49, 1980.

Scarf, F. L., and D. A. Gurnett, A plasma wave investigation for the Voyager mission, Space Sci. Rev., 21, 289, 1977.

Scarf, F. L., D. A. Gurnett, and W. S. Kurth, Jupiter plasma wave observations: An initial Voyager 1 overview, Science, 204, 991, 1979.

Scarf, F. L., D. A. Gurnett, and W. S. Kurth, Measurements of plasma wave spectra in Jupiter's magnetosphere, J. Geophys. Res., 86, 8181, 1981a.

Scarf, F. L., D. A. Gurnett, W. S. Kurth, R. R. Anderson, and R. R. Shaw, An upper bound to the lightning flash rate in Jupiter's atmosphere, Nature, 213, 684, 1981b.

Scarf, F. L., and C. T. Russell, Lightning measurements from the Pioneer Venus Orbiter, Geophys. Res. Lett., in press, 1983.

Smith, B. A., L. A. Soderblom, T. V. Johnson, A. P. Ingersoll, S. A. Collins, E. M. Shoemaker, G. E. Hunt, H. Masursky, M. H. Carr, M. E. Davies, A. F. Cook, II, J. Boyce, G. E. Danielson, T. Owen, C. Sagan, R. F. Beebe, J. Veverka, R. G. Strom, J. F. McCauley, D. Morrison, G. A. Briggs, and V. E. Suomi, The Jupiter system through the eyes of Voyager 1, Science, 204, 951, 1979.

Taylor, W. W. L., F. L. Scarf, C. T. Russell, and L. H. Brace, Evidence for lightning on Venus, Nature, 279, 614, 1979.

Thorne, R. M., and J. J. Moses, Electromagnetic ion-cyclotron instability in the multi-ion Jovian magnetosphere, Geophys. Res. Lett., 10, 631, 1983.

Tokar, R. L., D. A. Gurnett, and F. Bagenal, The proton concentration in the vicinity of the Io plasma torus, J. Geophys. Res., 87, 10,395, 1982a.

Tokar, R. L., D. A. Gurnett, F. Bagenal, and R. R. Shaw, Light ion concentrations in Jupiter's inner magnetosphere, J. Geophys. Res., 87, 2241, 1982b.

## FIGURE CAPTIONS

Figure 1 Frequency-time spectrograms showing examples of the whistlers detected by Voyager 1 as it traversed the Io plasma torus. a) Examples of whistlers from region A (see Figure 2). These whistlers have dispersions of about 300 $s\sqrt{Hz}$. b) Examples of region B whistlers with dispersions of about 50 $s\sqrt{Hz}$. c) Whistlers found in region C with dispersions of ~ 500 $s\sqrt{Hz}$.

Figure 2 Trajectory of Voyager 1 during its closest approach to Jupiter on 5 March 1979. Regions A, B, and C denote locations where whistlers were detected. The contours are a crude model of the electron plasma frequency in the Io plasma torus.

Figure 3 A summary of the whistler measurements used in this study. At the top, tics indicate the time of wideband frames which were available to search for whistler activity. The top panel shows the average frequency extent of whistlers detected within 40-s time intervals. The numbers indicate the number of whistlers included in the averages. Average dispersions are plotted in the bottom panel with error bars representing one standard

deviation. Whistlers from region A appear first near 300 $s\sqrt{Hz}$. Region B whistlers fall near 70 $s\sqrt{Hz}$ slightly later in time. The 500 $s\sqrt{Hz}$ whistlers near 1500 SCET are from region C.

Figure 4 A histogram showing the three populations of dispersions from the three groups of whistlers.

Figure 5 A spectrum accumulated over a 60 msec interval which shows a whistler at abour 4.5 kHz with an intensity of 39 $\mu Vm^{-1}$.

Figure 6 Whistler occurrence rates (per 48-s wideband frame) and broadband electric field strength integrated from 56 Hz to 10 kHz plotted as a function of time. The shaded region represents the dynamic range of the waveform receiver. The darkest shading indicates times when the receiver sensitivity falls below the peak whistler intensities.

Figure 7 Regions of whistler detection plotted against a model of the Io plasma torus. Analyses of whistler dispersions and integrated density along ray trajectories yield information on the source location of the whistlers.

Figure 8 Summary of the whistler source locations corresponding to the three regions where whistlers were detected. Results of nightside images of lightning activity are also shown [Cook et al., 1979].

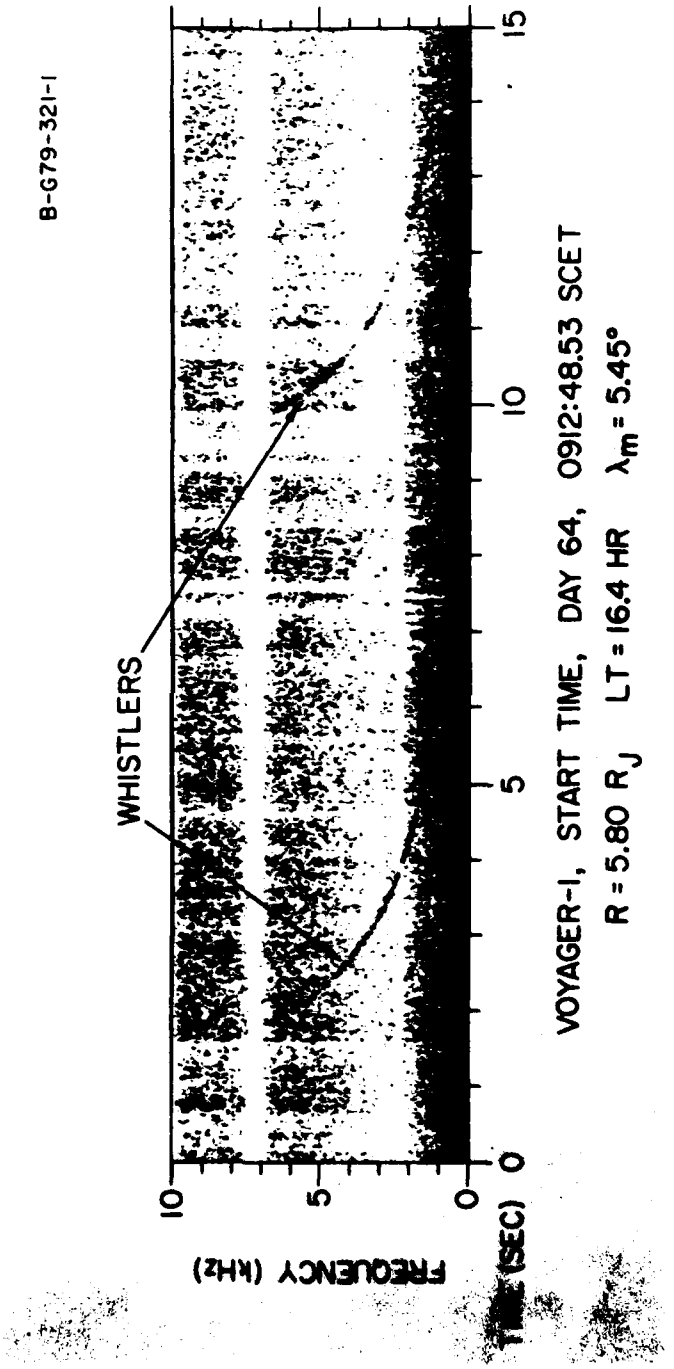
B-G79-321-1
WHISTLERS
VOYAGER-1, START TIME, DAY 64, 0912:48.53 SCET
R = 5.80 $R_J$ LT = 16.4 HR $\lambda_m$ = 5.45°
FREQUENCY (kHz)
10
5
0
0
5
10
15
TIME (SEC)

Figure 1a

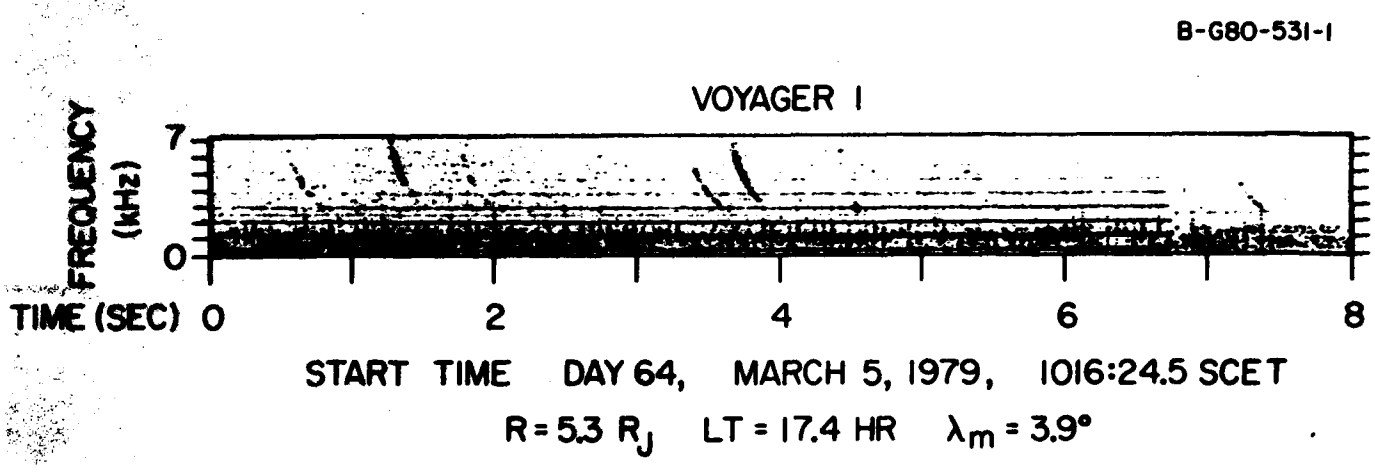
B-G80-531-1
VOYAGER 1
FREQUENCY (kHz)
7
0
TIME (SEC) 0
2
4
6
8
START TIME DAY 64, MARCH 5, 1979, 1016:24.5 SCET
R = 5.3 $R_J$ LT = 17.4 HR $\lambda_m$ = 3.9°

Figure 1b

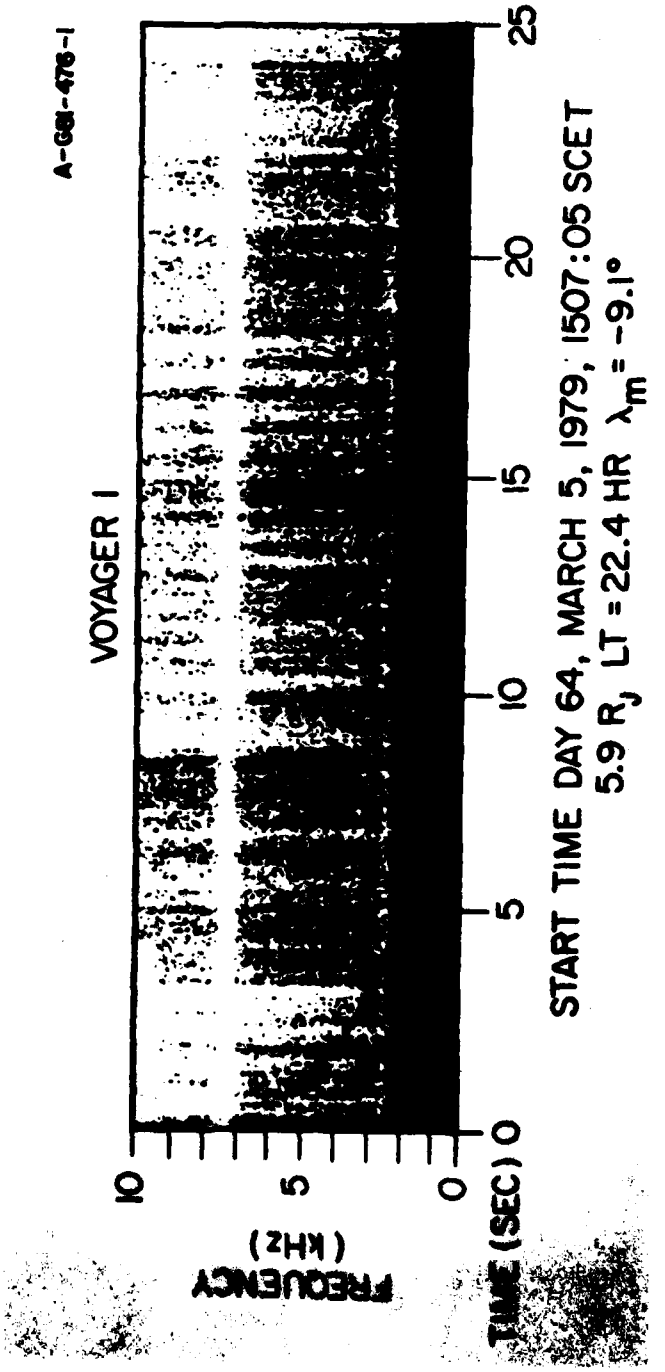
A-GBI-476-1
VOYAGER 1
START TIME DAY 64, MARCH 5, 1979, 1507:05 SCET
5.9 $R_J$ LT = 22.4 HR $\lambda_m$ = -9.1°
FREQUENCY (KHz)
TIME (SEC)
0
5
10
15
20
25

Figure 1c

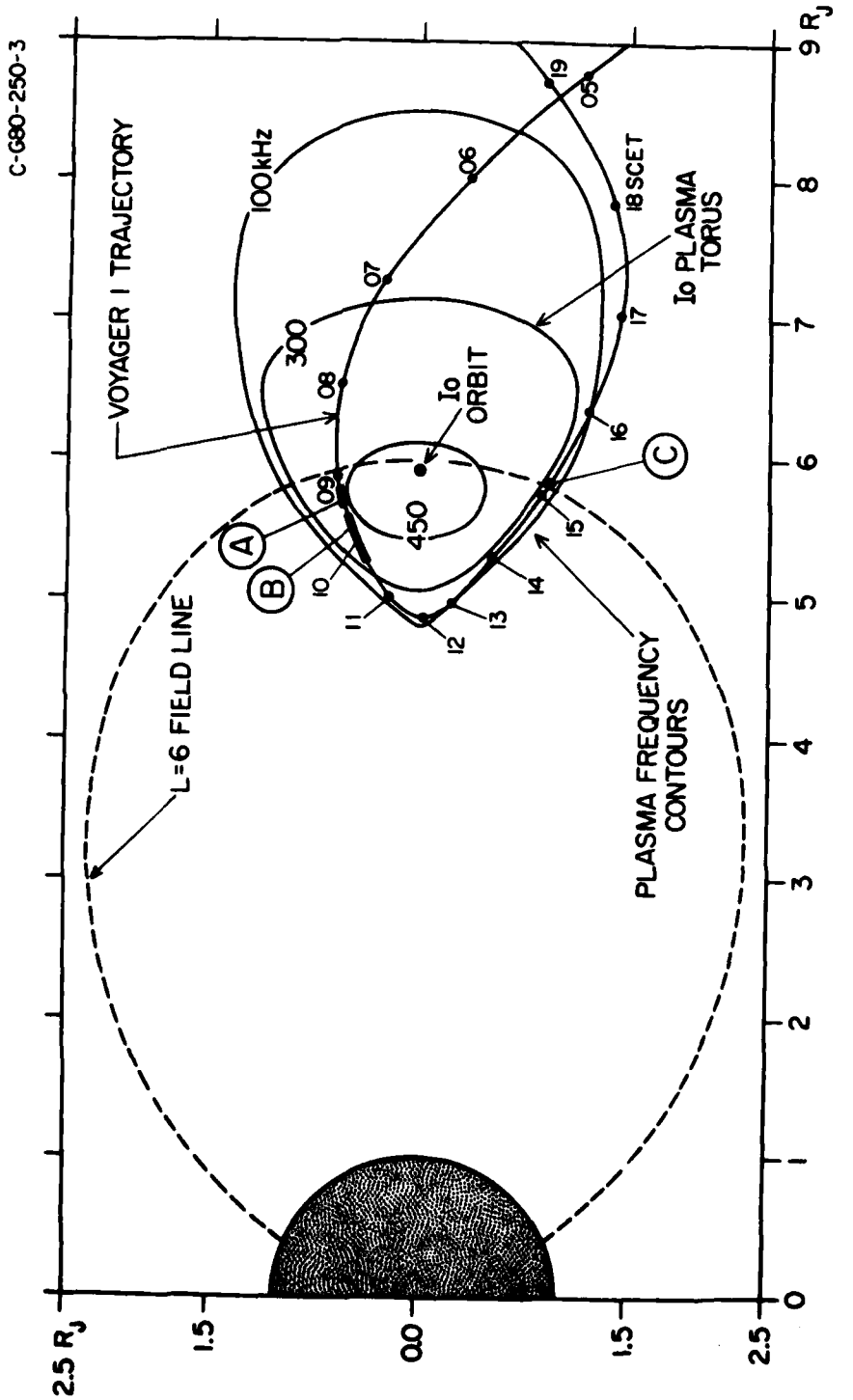
C-G80-250-3
VOYAGER I TRAJECTORY
100kHz
300
450
Io ORBIT
Io PLASMA TORUS
18 SCET
L=6 FIELD LINE
PLASMA FREQUENCY CONTOURS
A
B
C
2.5 RJ
1.5
0.0
1.5
2.5
9 RJ
0
1
2
3
4
5
6
7
8

Figure 2

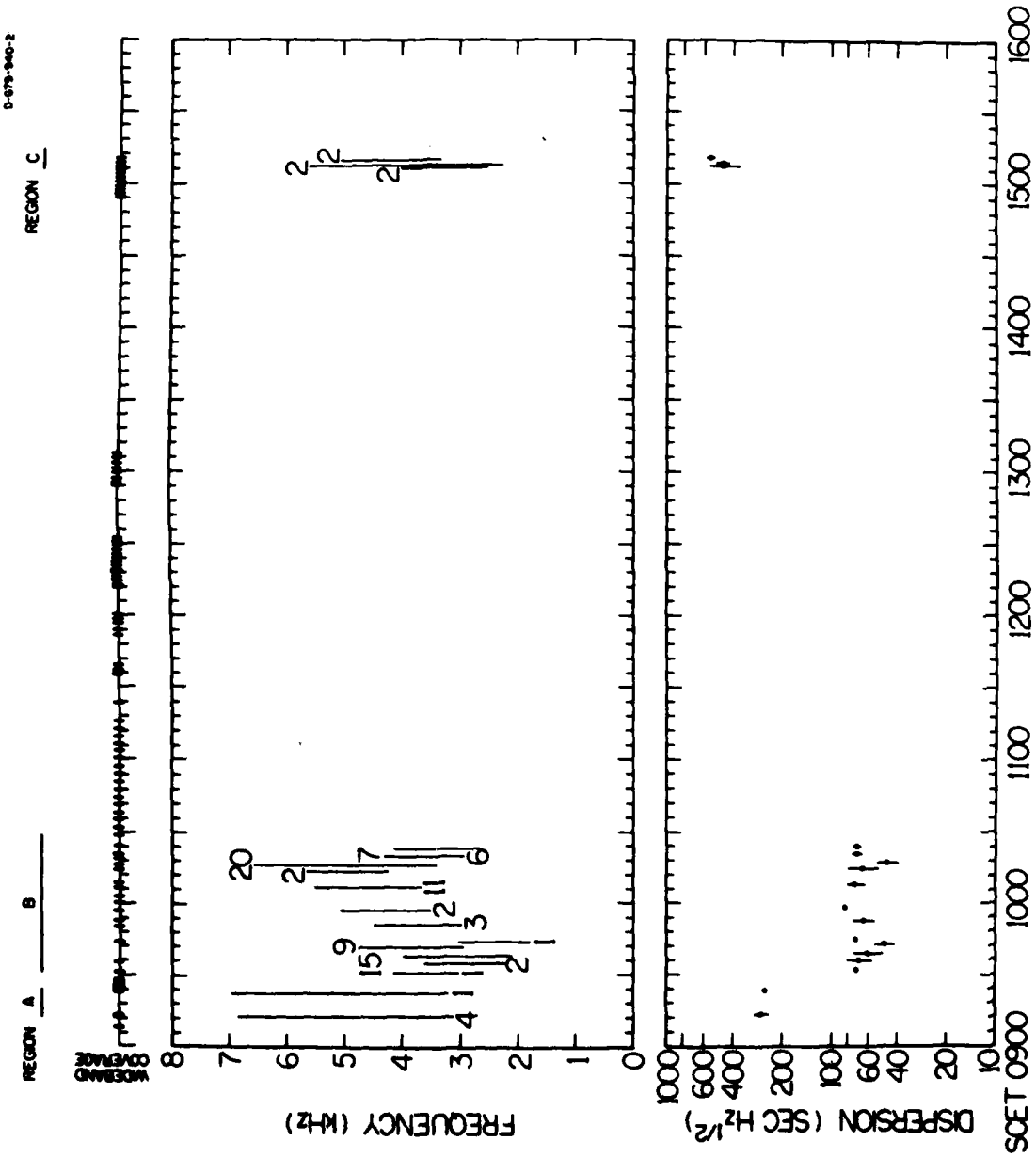
REGION A
B
REGION C
WIDEBAND OVERLOAD
FREQUENCY (kHz)
DISPERSION (SEC Hz$^{1/2}$)
SCET 0900
1000
1100
1200
1300
1400
1500
1600

Figure 3

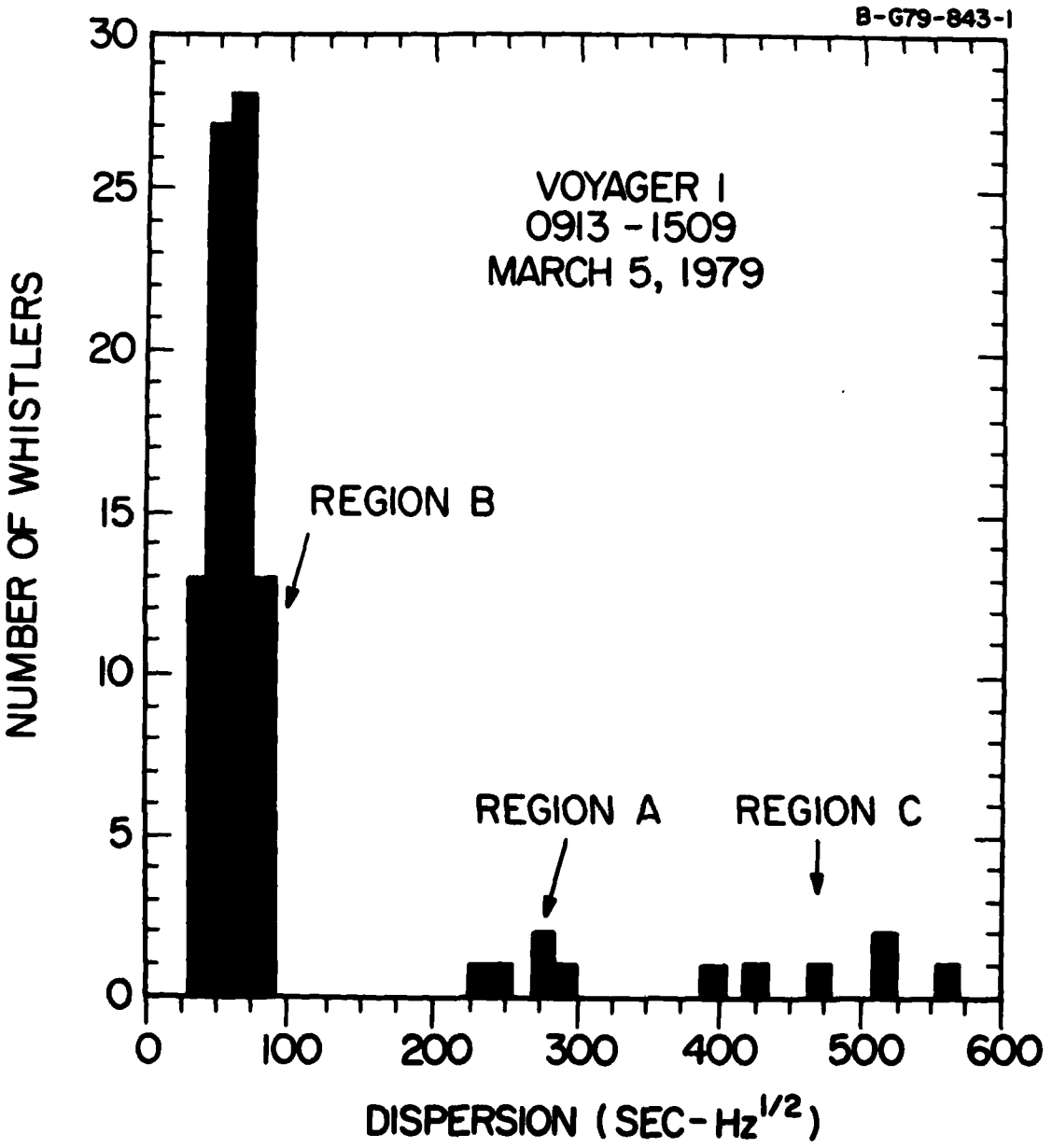
B-G79-843-1
VOYAGER 1
0913 - 1509
MARCH 5, 1979
REGION B
REGION A
REGION C
NUMBER OF WHISTLERS
DISPERSION (SEC-Hz^1/2)
0
5
10
15
20
25
30
0
100
200
300
400
500
600

Figure 4

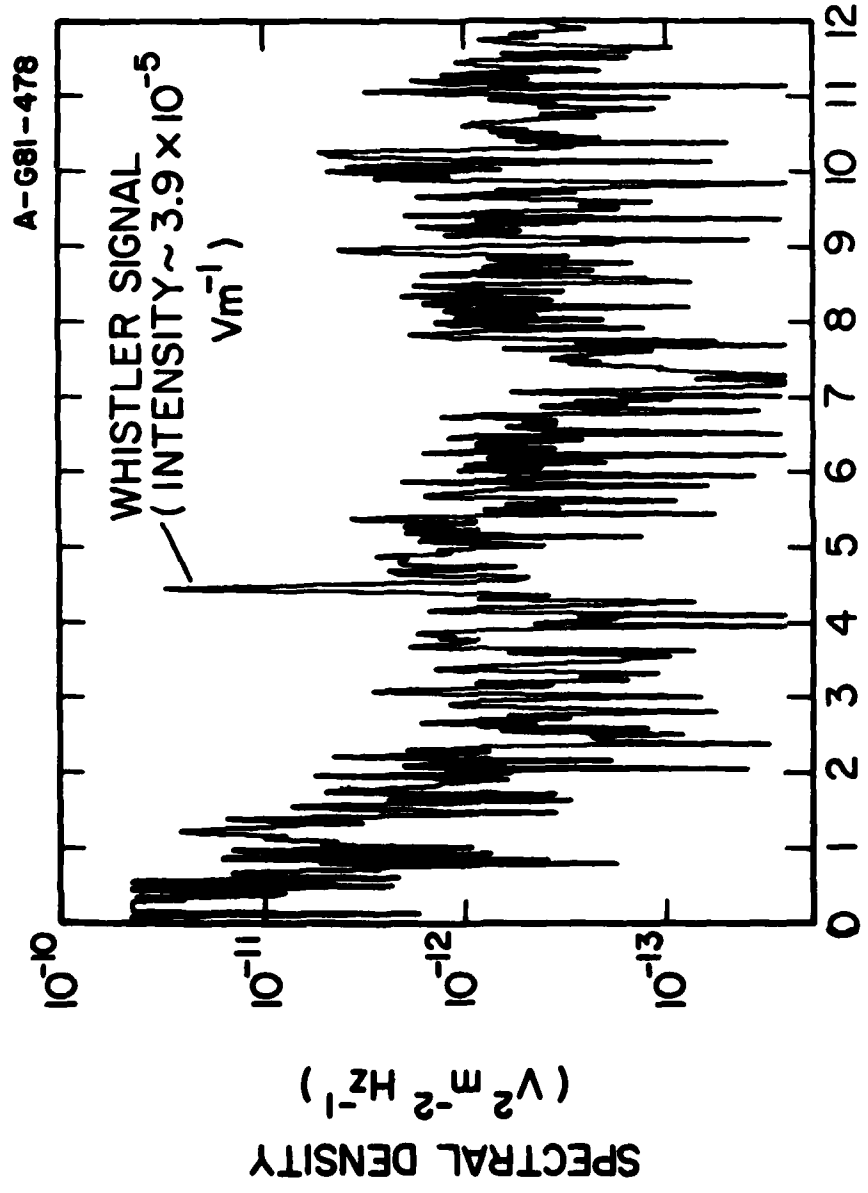


DAY 64, MARCH 5, 1979, 912:59.1 UT

REGION A, WHISTLER DISPERSION = 275 (SEC-Hz$^{1/2}$)

Figure 5

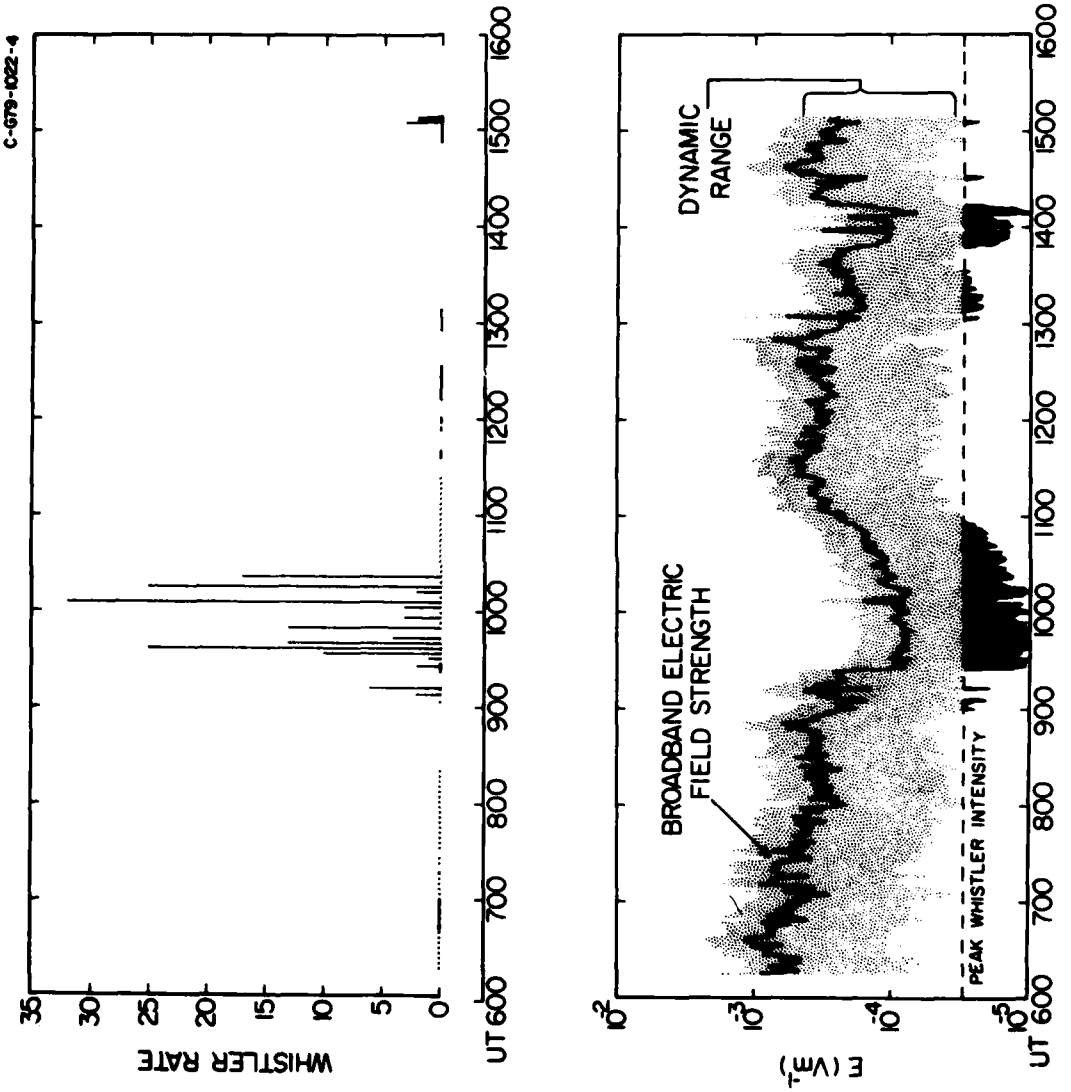
C-679-022-4
WHISTLER RATE
0
5
10
15
20
25
30
35
UT 600
700
800
900
1000
1100
1200
1300
1400
1500
1600
BROADBAND ELECTRIC FIELD STRENGTH
DYNAMIC RANGE
PEAK WHISTLER INTENSITY
E (V/m)
$10^{-2}$
$10^{-3}$
$10^{-4}$
$10^{-5}$

Figure 6

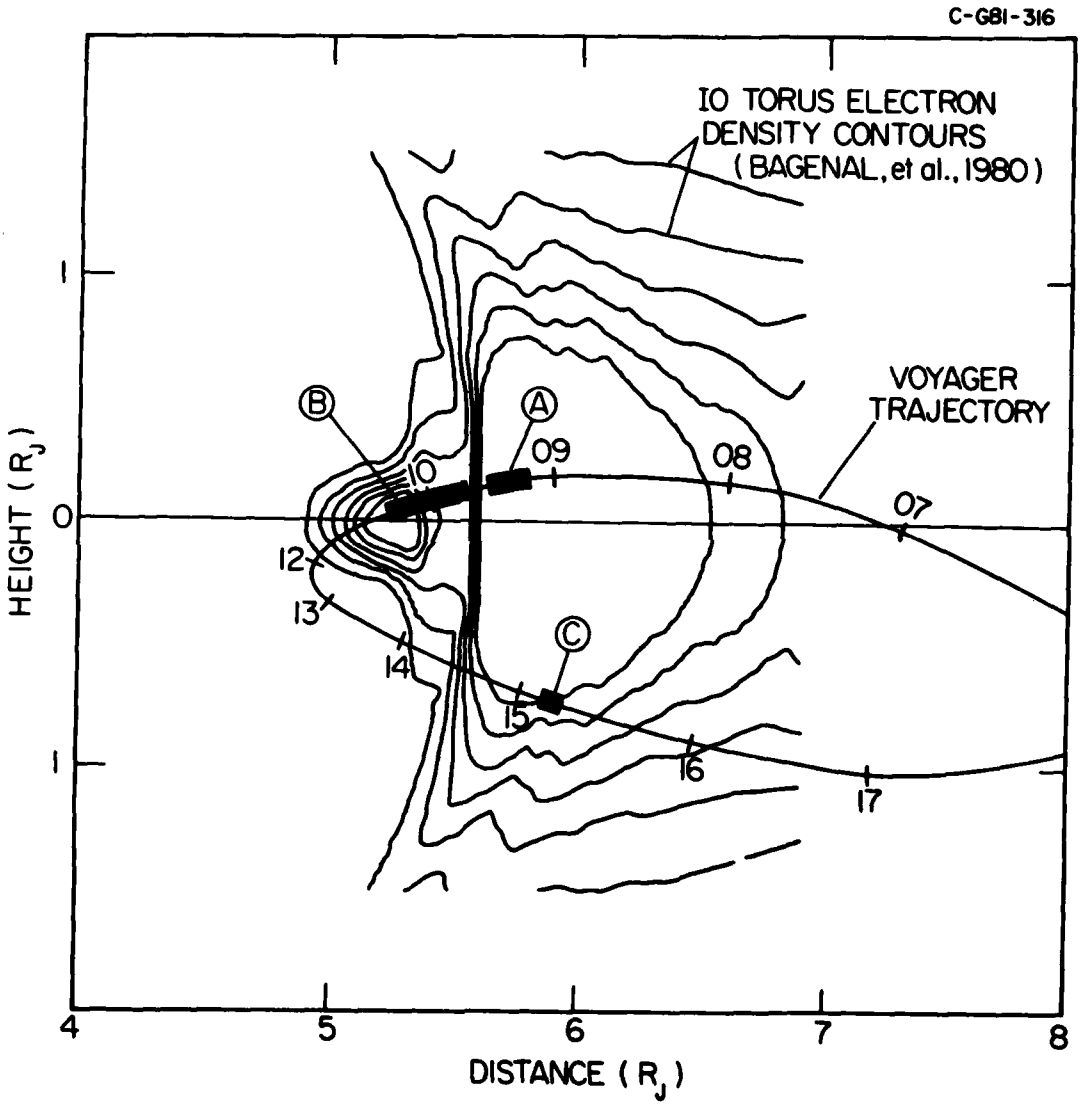
C-G81-316
IO TORUS ELECTRON
DENSITY CONTOURS
(BAGENAL, et al., 1980)
VOYAGER
TRAJECTORY
HEIGHT ( $R_J$ )
DISTANCE ( $R_J$ )
A
B
C
10
09
08
07
12
13
14
15
16
17
1
0
1
4
5
6
7
8

**Figure 7**

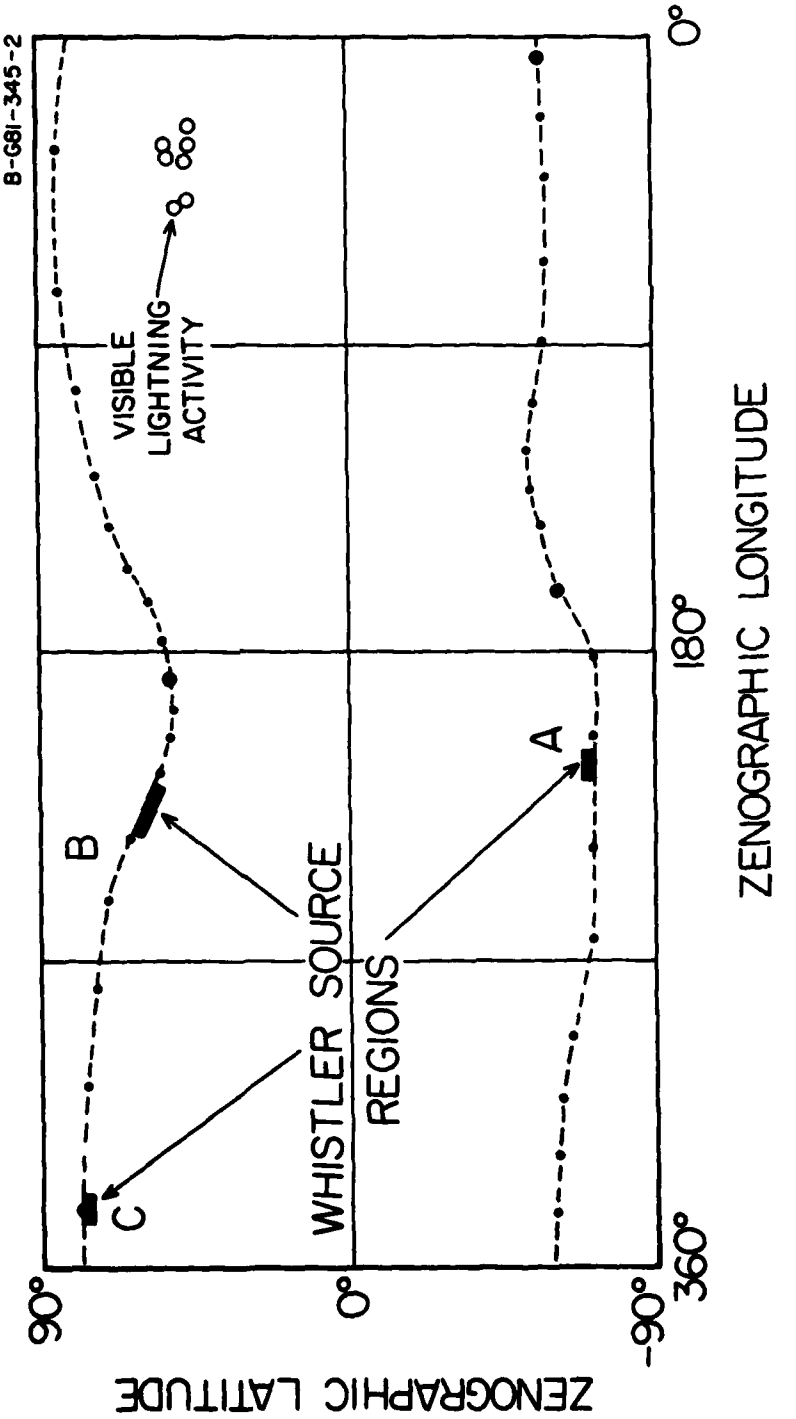
B-G81-345-2
VISIBLE LIGHTNING ACTIVITY
WHISTLER SOURCE REGIONS
A
B
C
90°
0°
-90°
360°
180°
0°
ZENOGRAPHIC LATITUDE
ZENOGRAPHIC LONGITUDE

Figure 8


DAT
FILM